



THE LONDON SCHOOL
OF ECONOMICS AND
POLITICAL SCIENCE ■

Experimental study of moisture content effects on the transient gas and particle emissions from peat fires

LSE Research Online URL for this paper: <http://eprints.lse.ac.uk/101298/>

Version: Accepted Version

Article:

Hu, Yuqi, Christensen, Eirik G, Amin, Hafiz M F, Smith, T. E. L. and Rein, Guillermo (2019) Experimental study of moisture content effects on the transient gas and particle emissions from peat fires. *Combustion and Flame*, 209. pp. 408-417. ISSN 0010-2180

<https://doi.org/10.1016/j.combustflame.2019.07.046>

Reuse

Items deposited in LSE Research Online are protected by copyright, with all rights reserved unless indicated otherwise. They may be downloaded and/or printed for private study, or other acts as permitted by national copyright laws. The publisher or other rights holders may allow further reproduction and re-use of the full text version. This is indicated by the licence information on the LSE Research Online record for the item.

Experimental study of moisture content effects on the transient gas and particle emissions from peat fires

Yuqi Hu^a, Eirik G. Christensen^a, Hafiz M.F. Amin^a, Thomas E. L. Smith^b, and Guillermo Rein^{a,*}

^a Department of Mechanical Engineering, Imperial College London, London SW7 2AZ, UK

^b Department of Geography and Environment, London School of Economics and Political Science, London WC2A 2AE, UK.

* Corresponding author. Email: g.rein@imperial.ac.uk; Tel: +44 (0) 20 7594 7036

Abstract

Peat fires are a global-scale source of carbon emissions and a leading cause of regional air quality deterioration, especially in Southeast Asia. The ignition and spread of peat fires are strongly affected by moisture, which acts as an energy sink. However, moisture effects on peat fire emissions are poorly understood in the literature. Here we present the first experimental work to investigate transient gas and particle emissions for a wide range of peat moisture contents (MCs). We include drying, ignition, smouldering spread, and even flaming stages. Peat samples conditioned to different MCs were burnt in the laboratory where a suite of diagnostics simultaneously measured mass loss rate, temperature profiles, real-time concentration of 20 gas species, and size-fractionated particle mass. It was found that MC affects emissions, in addition to peat burning dynamics. An increase in MC below a smouldering threshold of 160% in dry basis leads to a decrease in NH₃ and greenhouse gas emissions, including CO₂ and CH₄. The burning of wet peat emits more coarse particles (between 1 to 10 μm) than dry peat, especially during the ignition stage. In contrast, flaming stage emits mostly soot particles less than 1 μm, and released 100% more fully oxidised gas species including CO₂, NO₂ and SO₂ than smouldering. The examination of the resulting modified combustion efficiency (MCE) reveals that it fails to recognise with sufficient accuracy for smouldering combustion, especially for wet peat with MC >120%. MCE confuses drying and flaming, and has significant variations during the ignition stage. As a result, MCE

is not valid as a universal fire mode indicator used in the field. This work fills the gap knowledge between moisture and emissions, and provides a better understanding which can help mitigate peat fires.

Key words: wildfire; moisture; biomass; pollution; fire

1. Introduction

Peatlands are formed from the accumulation of partially decayed vegetation in water-logged environments over long time scales (centuries to millennia). Peatland ecosystems only cover ~3% of the Earth's land surface but are important terrestrial carbon pools, storing one-third of the world's soil carbon [1, 2]. Peatlands are vulnerable to smouldering fires: the slow, low-temperature, flameless burning of porous fuels, and the most persistent type of combustion [1, 3]. Smouldering peat fires are the largest fires on Earth (in terms of fuel consumption), they destroy soil ecosystems irreversibly and release more than 100 gas species and particles to the atmosphere [3-7].

Smouldering combustion is sustained by the heat released when oxygen directly attacks the surface of a solid fuel, whereas flaming combustion dominates when the oxidation takes place in the gas phase [3]. Black smoke plumes generated from flaming fires (homogenous combustion chemistry) are strongly buoyant, the diffusion flames move fast on the ground surface with a short residence time. In contrast, smouldering fires (heterogeneous combustion chemistry) persistently release weakly buoyant smoke plumes that accumulate near the ground surface (Figure 1) [2, 3]. This white-grey smoke is rich in particulate matter (PM) and can migrate long distances, causing regional haze crises, especially in Southeast Asia, Russia, and the USA [2, 8]. Inhalation of deleterious emission species such as carbon monoxide (CO), sulphur dioxide (SO₂) and PM can lead to various adverse human physiological responses, predominantly to the respiratory and cardiovascular systems [2].

Figure 1

Carbon dioxide (CO₂), CO, methane (CH₄) and ammonia (NH₃) are found to be the four predominant gas species emitted from peat fires [9]. Among these species, CO₂ and CH₄ are significant long-lived

greenhouse gases, while gases including CO, NH₃ and other non-methane organic compounds (NMOCs) impact atmospheric levels of CO₂ and CH₄ through photochemical processing [10]. On average, the annual carbon emissions from these fires are equivalent to a significant fraction of anthropogenic emissions, and create a positive feedback mechanism in the climate system [8, 11].

Peat moisture content (MC^1) can vary from 10 %, under natural drought conditions, up to > 300 %, when flooded [12, 13]. Peat moisture serves as an energy sink during a fire, and is the single most important property governing the ignition and spread of smouldering fires [3]. Natural droughts (e.g. El Niño) or anthropogenic drainages (e.g. for agriculture) lower the water table in peatlands, reduces the MC of the peat, and increases the frequency and extent of peat fires [1]. Once ignited, peat can sustain a smouldering fire, propagating horizontally and vertically through soil layers [3, 5, 14-17]. Preheating, drying, pyrolysis and oxidation are the sub-fronts forming the structure of a smouldering fire. Drying is not involved in chemical reactions and emits mainly water vapour [7, 18]. Most hydrocarbon (e.g., CH₄) emissions occur during peat pyrolysis, while CO, CO₂ and NH₃ are emitted by char oxidation [9]. Research investigating PM emissions from peat fire is limited to only a handful of studies, and PM formation mechanisms remain poorly understood [2, 19].

Mass flow rate ($g\ s^{-1}$) and emission factor (EF, the mass of species emitted per mass of dry fuel consumed, $g\ kg^{-1}$) are used in the literature to quantify fire emissions. EFs are also widely used in atmospheric sciences to determine the impacts of fire in the context of global climate change [2]. Rein et al. [7] and Hadden [20] studied the mass flow rates and EFs from peat fires for CO₂ and CO. Hu et al. [9] recently found that the transient gas and particle emissions and their EFs are significantly dependent on combustion dynamics. These studies [7, 9, 20] are laboratory-based which simplify the vast complexity of natural conditions found in peatland ecosystems, but provide vital insights into emission and peat fires. Field studies provide invaluable data from landscape-scale fires [6, 19, 21] but are most challenging to study due to natural heterogeneity [15, 21]. Field scientists stress the need for controlled laboratory studies to test hypotheses generated from limited field observations [19].

¹ Moisture content of peat is defined as the mass of water divided by the mass of a dried sample (expressed as %).

Fundamental understanding from laboratory-scale experiments can be extrapolated and applied to field-scales to provide context and a better understanding of field data. Research is therefore needed at all scales to advance the understanding of peat fire phenomena [15].

In this work, gas and particle emissions from smouldering peat were measured in the laboratory under different moisture conditions. This allowed the effects of MC on the transient emissions to be investigated for the first time. This work also examined drying (i.e. without a source of ignition) and flaming peat, which is rarely compared to smouldering, providing a unique and comprehensive understanding of the emission from different fire stages.

2. Experimental method

A commercially available temperate Irish sphagnum peat was used in the experiments, this pre-milled peat has homogeneous properties and composition, and has been used in previous smouldering studies [9, 13, 14]. Elemental analysis (dry basis) shows that the mass fraction of C/H/N/S of this peat is 54.1/5.1/1.3/0.5 %, respectively. Peat samples were conditioned to different MCs values prior to a series of flaming, smouldering and drying experiments, following the same drying and rewetting protocol used in [9, 13- 15]: raw peat was firstly oven dried at 80 °C until no further mass loss was observed; next, the dry peat was rewetted with a corresponding amount of water to achieve a series of desired MCs. The sample was then mixed thoroughly and left in a sealed bag for 48 h for moisture equilibrium. For smouldering peat experiments, the targeted MC values were: dry peat, 25%, 50%, 75%, 100%, 120%, 140%, 160% and 180%. An absolute 0 % MC peat is not possible as once dry peat finds air, it quickly absorbs the ambient moisture [14]. Following the peat MC verification protocol developed in [15], the actual MCs of the conditioned samples were determined to be: 1.5 ± 0.9 % (dry peat); 26.7 ± 0.8 %; 54.5 ± 1.0 %; 78.2 ± 2.2 %; 103.0 ± 1.1 %; 125.4 ± 2.5 %; 142.9 ± 3.0 %; 158.7 ± 2.4 % and 177 ± 2.0 %, respectively. Dry peat samples were used for flaming experiments. 180 % MC samples were used for drying experiments. Before starting an experiment the sample was again vigorously mixed to remove moisture gradients (< 1.9 %, as measured) [15].

Peat fire experiments were carried out on a comprehensive fire emission experimental rig characterised in a previous study [9]. Two different open-top reactors (burning Reactor “A” and drying Reactor “B”) were used (Figure 2). Both reactors have an inner dimension of 20 cm by 20 cm in cross section and 10 cm in depth, ensuring a fixed peat volume used in each experiment. Reactor A, used for both smouldering and flaming experiments, was built from 1.3 cm thick mineral fibre board with a coil heater buried 5 cm along one side of the reactor below the free surface [9, 14, 15]. For reactor B used in drying experiments, the difference is that the bottom wall is made of a 1 mm thickness aluminium sheet facilitating heat conduction from a hot plate placed underneath.


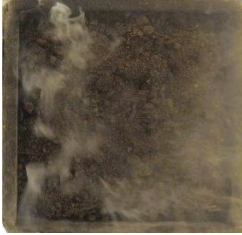

Figure 2

Emissions from the drying, smouldering and flaming peat were collected using an inverted fume hood and transported into a duct where a fan controls the extraction rate [9]. Flow inside the emission duct was well mixed. The extraction rate was set to $0.035 \text{ m}^3 \text{ s}^{-1} \pm 2.5 \%$ because it ensured all emissions were collected, while minimizing flow perturbations to open combustion [9]. Following the ignition protocol used in [5, 9, 14, 15], the ignition of the peat sample in the experiments was achieved by applying 100W of power to the coil for 30 min.

Flaming peat is not frequently observed in the natural environment (and is even less often studied in the literature) because its occurrence requires unusual thermodynamic conditions and enhanced oxygen supply (e.g., strong winds) [3, 11]. The ignition coil for flaming experiments was kept on at all times to encourage the production of pyrolysate emission which can feed homogeneous gas-phase oxidation flames [3, 22]. Maintaining a steady and relatively long-lasting flaming peat (> 3min) was necessary so that valid data could be collected. When increasing the extraction rate to $0.105 \text{ m}^3 \text{ s}^{-1} \pm 2.0 \%$, surface peat glowing was observed 20 min from turning the ignitor on. A small pilot flame was used to ignite the pyrolysate, and a steady and relatively long-lasting (~5 min) flaming peat was obtained. When we decreased the extraction rate, however the flame was disrupted, and the data could not be collected for long enough. As a result, $0.105 \text{ m}^3 \text{ s}^{-1}$ is the lower value possible for flaming peat in this rig.

Emissions from drying peat was studied by fixing the temperature of the hot plate to 95 ± 1 °C. At least 3 replicate smouldering experiments were carried out for each MC condition, and both flaming and drying experiments were repeated twice. Table 1 provides a summary of all the experiments.

Table 1 Summary of the experimental configuration of peat drying, smouldering and flaming. Top view images of the experiments are shown. The peat was ignited at the left side, and propagated to the right.

	Drying	Smouldering	Flaming
Peat moisture content	180%	0% - 180%	0% (dry peat)
Emission extraction rate	$0.035 \text{ m}^3 \text{ s}^{-1}$	$0.035 \text{ m}^3 \text{ s}^{-1}$	$0.105 \text{ m}^3 \text{ s}^{-1}$
Ignition coil	n/a	100 W for 30 min [9, 14]	100 W, always on
Pilot flame	n/a	n/a	1s, at 20 min
Hot plate	95 °C, always on	n/a	n/a
Visual example			

This work uses the same diagnostics for measuring burning dynamics (mass loss, temperature profiles, visual and infrared images) and transient emissions (gas concentration, particle mass) used in [9]. 20 different gas species which are most abundant and important from the literature were measured using a Thermo Scientific Nicolet iG50 Fourier-transform infrared (FTIR) spectroscopy: CO₂, CO, CH₄, NH₃, acetylene (C₂H₂), ethylene (C₂H₄), ethane (C₂H₆), propylene (C₃H₆), propane (C₃H₈), butane (C₄H₁₀), methanol (CH₃OH), formaldehyde (CH₂O), nitric oxide (NO as NO_x), nitrogen dioxide (NO₂), hydrogen cyanide (HCN), acetic acid (CH₃COOH), acetaldehyde (C₂H₄O), formic acid (CH₂O₂), hydrogen chloride (HCl), and SO₂. The operation of the FTIR follows ISO 19702 to minimise the water interference of the results: water spectra for different concentrations were calibrated and used to correct the spectra of desired species; all ducts of the FTIR were constantly heated to 100 °C to avoid gas condensation; a thorough purging of the FTIR system using pure nitrogen was carried out before and after each experiment. Species' background concentrations were subtracted from the results.

Size-fractionated particles ($D \geq 10 \mu\text{m}$; $2.5 \mu\text{m} \leq D \leq 10 \mu\text{m}$; $1 \mu\text{m} \leq D \leq 2.5 \mu\text{m}$; $D \leq 1 \mu\text{m}$) which went through very short smoke aging ($< 3\text{s}$) inside the duct of the rig were collected using an isokinetic probe and a Dekati 4-stage PM cascade impactor, in accordance with ISO 23210, for 10 min after every 2 hrs [9]. The masses of PM_{10} (particle aerodynamic diameter $\leq 10 \mu\text{m}$), $\text{PM}_{2.5}$ ($\leq 2.5 \mu\text{m}$) and PM_1 ($\leq 1 \mu\text{m}$) from each measurement slot were calculated from the mass gain of the size-fractionated particles weighted using a 0.01 mg resolution Sartorius balance.

3. Results and discussion

3.1 Burning dynamics

Figure 3 shows the evolution of mass loss rate (MLR) from peat flaming, smouldering and drying. The MLR from the short flaming fire ($0.057\text{-}0.073 \text{ g s}^{-1}$) was on average 325% greater than that of smouldering peat, indicating a more intense combustion process [3]. In this work, two general combustion stages were used to describe the evolution of a smouldering peat fire: ignition stage (first 30 min with coil heater on) and spread stage [9]. Smouldering peat with MCs of 0%, 75% and 160% were chosen to represent the typical MLR trends exhibited within the whole MC range.

Figure 3

For peat with a MC $< 160\%$, self-sustained smouldering was observed after the ignition stage for all repeats. We determine self-sustained smouldering from a steady increase of the MLR. When the MC was increased to 160%, two out of the four repeats failed to show self-sustained smouldering. None of the 180% MC peat samples self-sustained. Consequently, for our samples, 160% is deemed to be the critical smouldering MC threshold, as defined in [3, 12]. The value of 160% is higher than the values reported in previous literature which are in the range of 110%- 150% [5, 14, 23]. The MC threshold exists because moisture leads to heat losses by evaporation, while density, thermal conductivity, and the heat of char oxidation also affect the MC threshold [12]. The lower dry bulk density (224 kg m^{-3}) and inorganic content (2.5%) of the peat used in this work result in higher oxygen permeability and lower

thermal inertia than the peat used in previous studies (for example, peat used in [5] has a dry bulk density of 430 kg m^{-3} and an inorganic content of 8%). As a result, the decreased heat losses and increased oxygen supply move the critical MC towards the higher value we observed here [12].

Figure 4 shows that MC significantly affects fire dynamics. This unique comparison of peak MLR of flaming, smouldering and drying reveals the difference among fire stages. The MLR of flaming peaks at 0.073 g s^{-1} , while the peak MLR of smouldering decreases linearly with MC (from 0.054 g s^{-1} for dry peat, to 0.027 g s^{-1} at 160% MC). The MLR of drying is of one magnitude lower than flaming and smouldering, peaking at 0.005 g s^{-1} .

Figure 4

Temperature profiles of the experiments show the spread of a fire. By tracking the drying front ($100 \text{ }^\circ\text{C}$ isotherm) as a marker [9, 14], the lateral spread rate of smouldering across the reactor [14, 17] was studied. Figure 5 presents the first systematic investigation of the MC effects on smouldering spread rate which is controlled by the oxygen supply and heat transfer [3]. This data reveals a negative linear relationship between spread rate and MC, corresponding with review of Santoso et al. [17] which collected fire spread data gathered from different sources in the literature. As the MC increases, the spread rate becomes less sensitive to depth. When the peat becomes wet ($\text{MC} > 50\%$), smouldering spreads faster beneath the free surface, leading to the formation and collapse of an overhang [14]. For $\text{MC} > 75\%$, the $100 \text{ }^\circ\text{C}$ isotherm never appears on the top layer.

Figure 5

Averaging all smouldering experiments that ignited, the mean lateral spread rate is $3.0 \pm 1.5 \text{ cm h}^{-1}$. Santoso et al. [17] reported a very similar lateral spread rate ($3.1 \pm 1.1 \text{ cm h}^{-1}$) for peat with a large MC span (from 5% to 150%). Data and comparison confirms that smouldering is a very slow burning fire [3], and its spread rate is two orders of magnitude lower than the spread of flaming fire [8].

3.2 Transient gas emissions

There is a lack of gas concentration data from peat fire in the literature. Figure 6 shows the transient excess CO₂ concentrations ([CO₂]) from flaming, smouldering and drying stages. [CO₂] from flaming ranged between 460 and 864 ppm, while smouldering and drying ranged within 900 and 5 ppm, respectively. Generally, the evolution of [CO₂] at the spread stage of a smouldering fire follows the MLR trends reported in [9]. [CO₂] decreases with the MC, which is partly attributed to the added water decreasing the dry mass of fuel (decreasing dry peat bulk density with MC). This effect was studied in detail in [13, 14]. For example, for 0% MC, the dry bulk density of peat is 220 kg m⁻³, and decreases to 102 kg m⁻³ for our 160% MC (Fig. S1). Fig. S2 shows the transient concentrations of 20 analysed gas species from all experiments.

Figure 6

The gas species CO₂, CO, CH₄, NH₃ and HCN were selected for analysis in Figure 7-9 because of their higher EFs and health effects [2, 9, 15]. For smouldering experiments, the moisture effects were investigated under the ignition and spread stages.

Figure 7 shows the peaks of [CO₂] and [CO] from all experiments. Generally, the concentrations of the species that are mainly emitted from char oxidation (e.g., CO and CO₂) peak simultaneously with MLR at the spread stage [9]. The time to reach these peaks increased with MC. A 25% increase of the MC leads to a 45% and 64% decrease of the peak [CO₂] and [CO], respectively. The CO to CO₂ ratio (CO/CO₂), an index of the incompleteness of combustion [3], ranges between 0.26- 0.51 for smouldering, contrasting with 0.04 CO/CO₂ for flaming. No CO was detected during drying.

Figure 7

Species that are mainly generated from peat pyrolysis (e.g., CH₄) have concentrations that peak at the ignition stage (Figure 8 (a)) for all smouldering experiments. Peak [CH₄] at MC < 140% is at least 130%

larger than those from flaming peat. A 25% increase of MC from dry peat leads to a 52% decrease of the peak [CH₄]. No CH₄ was detected during peat drying.

In contrast with the results for CH₄, [HCN] were higher from smouldering spreading than ignition (Figure 8 (b)). During the smouldering spread stage, peak [HCN] stayed relatively constant at 0.5 ppm with MC < 75%, and decreased gradually for MC > 75%. Negligible HCN (<0.08 ppm) was detected during flaming peat, and no HCN was detected during peat drying.

Figure 8

In [9], it was proposed NH₃ could be a candidate atmospheric marker for smouldering peat fires because of their disproportionately larger EFs compared with flaming forest fires (20 times). Figure 9 shows the peak [NH₃] found in these experiments. On average, [NH₃] from smouldering peat is 14 times larger than those for flaming. This further demonstrates that NH₃ is a very strong indicator for smouldering. [NH₃] measured during the smouldering spread stage were at least 5.5 times higher than those from the ignition stage, verifying that NH₃ is not formed through peat pyrolysis and NH₃ is a by-product of char oxidation [7, 9]. No NH₃ was detected during peat drying.

Figure 9

Mass flow rate of gas emissions had been investigated in a handful of previous studies [7, 9, 20]. In this work and [9], the excess mass flow rate of species *i* (\dot{m}_i'' , g·s⁻¹) is calculated from burning peat ($\dot{m}_{i,f}''$) and the air entrainment ($\dot{m}_{i,a}''$). \dot{m}_i'' is given by the species density (ρ_i , ideal gas assumption, g m⁻³), the total volume flow rate (\dot{V} , m³·s⁻¹), and the total concentration of the species ($[i]_t$, ppm) in the exhaust duct.

$$\dot{m}_i'' = \dot{m}_{i,a}'' + \dot{m}_{i,f}'' = \rho_i [i]_t \dot{V} \quad (1)$$

The mass flow rate of species *i* by air entrainment is given by the concentration of the species in the entrainment air ($[i]_a$), the forced volumetric flow rate without fire (\dot{V}_a) and the species density.

$$\dot{m}_{i,a}'' = \rho_i [i]_a \dot{V}_a \quad (2)$$

Prior to ignition, we measured background gas concentration in the air so the excess contribution from the fire ($[i]$) is:

$$[i] = [i]_t - [i]_a \quad (3)$$

We also ran experiments measuring the volumetric flow rate before and after the ignition. Because of the low buoyant nature of smouldering plumes, the flow rate is the same as without fire:

$$\dot{V}_a = \dot{V} \quad (4)$$

From Equation 1, the mass flow rate of species i from peat burning can be calculated by:

$$\dot{m}_{i,f}'' = \rho_i [i]_t \dot{V} - \dot{m}_{i,a}'' = \rho_i [i] \dot{V} \quad (5)$$

Normalising the mass flow rate of species i per unit length (L, m), width of our reactor, the linear mass flux ($\text{g s}^{-1} \text{m}^{-1}$) of all 20 gas species was calculated. The uncertainty of mass flux is estimated at $\pm 12.5\%$ in [9]. Fig. S3 shows the transient mass fluxes of CO_2 , CO , CH_4 , HCN and NH_3 from all experiments. With an extraction rate of $0.105 \text{ m}^3 \text{ s}^{-1}$, CO_2 mass flux of flaming peat reached $0.8 \text{ g s}^{-1} \text{m}^{-1}$, distinctly larger than those measured during smouldering which ranged between $0.06\text{-}0.3 \text{ g s}^{-1} \text{m}^{-1}$. This is because smouldering is an incomplete combustion process where a large fraction of carbon gases are emitted without being fully oxidised into CO_2 [3]. For smouldering, the mass flux of CH_4 can reach up to $8 \text{ mg s}^{-1} \text{m}^{-1}$. The peak mass fluxes of deleterious CO , HCN and NH_3 measured during smouldering ranged between $16\text{-}54 \text{ mg s}^{-1} \text{m}^{-1}$, $0.04\text{-}0.08 \text{ mg s}^{-1} \text{m}^{-1}$, and $0.2\text{-}2 \text{ mg s}^{-1} \text{m}^{-1}$, respectively, posing acute respiratory and cardiovascular risks to exposed populations [2].

By assuming that the moisture evaporation rate corresponds to the MC of the peat, the transient EF calculated from a mass loss approach was validated in [7, 9]. This work follows the same assumption of moisture emission and the EF mass loss approach (Equation 6) to calculate the transient EF of different gas species i ($EF_i(t)$, $\text{g} \cdot \text{kg}^{-1}$ dry mass burnt).

$$EF_i(t) = \frac{\dot{m}_{i,f}''}{\left(\frac{\dot{m}}{1+\varphi_\omega}\right)} \quad (6)$$

Where \dot{m} is the transient MLR of the sample (g s^{-1}), φ_ω is the MC of the sample in dry basis (%).

The transient EF is a function of both mass flux and MLR, these two quantities do not peak simultaneously, and thus the peak EF and MC does not have conclusive trends with time. The transient EFs of CO₂, CH₄ and NH₃ from smouldering peat with MCs of 0%, 75% and 160% are shown in Figure 10 as examples of the trends exhibited across all MC ranges. We find that MC affects the EFs of different gas species: the transient EFs of CO₂, CH₄ and NH₃ clearly decrease with the increase of MC. An increase of 160% MC from dry peat led to 48%, 82%, and 84% decrease of the CO₂, CH₄ and NH₃ EFs, respectively. The decreasing CO₂ EF with MC found here contradicts the findings of [7] who found an increasing trend in assisted burning. The decreasing EF trend for CH₄ measured here with MC is well-explained by the theory that peat at low moisture smoulders with a stronger pyrolysis front, releasing a larger fraction of non-fully oxidised carbon species [7].

Figure 10

Wet peat (75% or 160% MC) emits more CO and HCN than dry peat. The increasing CO EF with MC contradicts the findings of [7] who found in thermally assisted experiments that CO transient EFs are independent of the moisture. Given that the evolution of EF varies among gas species, it is likely that MCs affect all burning dynamics. For example, the opposed trends for CO₂ and CO EFs with MC can be explained by the important roles of heat transfer and oxygen supply in controlling emissions. CO/CO₂ ratio is known to decrease with the strength of combustion, so these trends can be explained by the decrease of combustion strength with MC (see Fig.S4) [3, 7].

Figure 11

By comparing the EFs before and during flaming stage, signals that are unique to peat gaseous pyrolysate oxidation were discovered: species including CO₂, C₂H₂, CH₂O, NO, NO₂, SO₂ and CH₃COOH experienced a distinct increase during flaming. For example, the EF of CO₂ increased ~513%, and NO EF increased ~ 156%. In contrast, a clear decrease of CO, CH₄, C₂H₆, C₃H₈ and C₄H₁₀

was observed during flaming. For example, the EF of CO declined ~46% during flaming, and CH₄ decreased ~70%. C₂H₄, C₃H₆, CH₃OH, HCN, C₂H₄O, CH₂O₂ and HCl showed negligible differences before and during flaming and were thus deemed insensitive to changes in combustion regimes.

3.3 Transient particle emissions

Particle emissions (PM₁₀, PM_{2.5} and PM₁) from peat flaming, smouldering and drying experiments were gravimetrically measured. Typical size-fractioned particles collected from the PM impactor are shown in Figure 12. Blackish sooty particles with a diameter less than 1 µm were observed from flaming peat, which accounts for ~92% of the total particles. In contrast, PM₁ collected from smouldering were yellowish and contained negligible black carbon, which is characteristic for haze aerosols [2]. For smouldering peat, PM₁ from spread stage took up 67 ± 3% of all the detectable particles, similar to [9], while the ignition stage generated far less PM₁ (2.2 ± 0.6%). No PM was detected during the drying experiments.

Figure 12

The linear mass fluxes of PM species j (\dot{m}_j , mg·s⁻¹·m⁻¹) were calculated using Equation (7).

$$\dot{m}_j = \frac{m_j}{\Delta t L} \cdot \frac{\dot{V}}{\dot{V}_j} \quad (7)$$

Where m_j is the time-resolved mass of sampled PM (mg); Δt is the time interval of a measurement (s); \dot{V} is the volumetric flow rate in the duct; \dot{V}_j is the PM sampling flow rate in the impactor (0.5 dm³ s⁻¹ ± 5.0%); L is the width of the reactor (m).

Fig. S5 shows the linear mass fluxes of PM₁₀, PM_{2.5} and PM₁ between smouldering dry peat (0% MC) and wet peat (75% MC). Generally, the evolution of PM mass fluxes follows the trend of MLR [9], and both samples reached ~ 4.0 mg s⁻¹ m⁻¹ PM₁₀ during spreading stage. In contrast, flaming emits 2.4 times more PM₁₀.

Following the same calculation method used in [9], the transient EF of PM species j ($EF_j(t)$, g kg⁻¹ dry mass burnt) from the experiments were determined using Equation (8):

$$EF_j(t) = \frac{m_j}{\frac{m_{\Delta t} - m}{(1 + \varphi_\omega)}} \cdot \frac{\dot{V}}{\dot{V}_j} \quad (8)$$

Where m and $m_{\Delta t}$ are the mass of the wet peat before and after each PM measurement interval (10 min every 2 h) (mg); φ_ω is the MC of the peat sample in dry basis (%).

We presented the EFs of flaming particles for the first time, with PM₁ (28 g kg⁻¹) comprising 93 ± 1.8 % of the total particles. It is worth noting that C₂H₂, a precursor species of soot [24], experiences a distinct increase during flaming. Figure 13 shows significant variations of PM EFs between the ignition and spread stages from dry and wet peat. Wet peat emits more particles during ignition, and 54 ± 3.2% of them are between 1 and 2.5 μm in diameter. In contrast, 52 ± 1.7 % of the particles from the ignition stage of dry peat are in the range of 2.5 to 10 μm in diameter.

Figure 13

The transient EF of PM follows the evolutions of MLR during the spread stage. This trend was also observed in previous experiments by Hu et al. [9] for a 100% MC peat. Roulston et al. [19] showed in the field a declining PM EFs through time. The peak EF of PM_{2.5} during the spread stage in [9] and this study are both ~ 20 g kg⁻¹, causing deterioration of air quality and human health [2].

3.4 Modified combustion efficiency

Modified Combustion Efficiency (MCE) is a variable widely used in the atmospheric literature to describe the combustion regimes (e.g., smouldering vs. flaming) of biomass burning [10, 20]. It is calculated from the excess mole fraction (Δ , the mole fraction of species in the smoke, with mole fractions from the background air subtracted) of CO₂ and CO (Equation 9) [10, 25].

$$MCE = \frac{\Delta CO_2}{\Delta CO + \Delta CO_2} \quad (9)$$

There are discrepancies in terms of the use of MCE from the literature. Stockwell et al. [6] deemed that a high MCE ~0.99 indicates flaming, and a fire-averaged MCE between 0.75 and 0.84 indicates smouldering; Akagi et al [25] proposed that smouldering MCE is most often near 0.8, and an overall MCE near 0.9 suggests approximately equal amounts of flaming and smouldering. However, a review

of the use of MCE in field studies [2] shows that it is partially misunderstood and highly sensitive to unknown field variables. A recent laboratory study [9] found that MCE fails to capture the transient combustion dynamics of a smouldering peat fire. In this work, the MCE calculated from flaming and smouldering was examined in depth and for the first time compared to drying.

Figure 14 shows the transient MCE from all experiments. Flaming has a generally high MCE ranging from 0.91 to 0.98 with an average of 0.96, in agreement with [6]. For smouldering peat experiments, the mean MCE decreases gradually from 0.79 for dry peat to 0.67 for wet peat. The decrease of MCE with MC indicates a low combustion efficiency at high moisture conditions. However, the averaged MCE for $MC > 25\%$ was found to stay below 0.75, in disagreement with the lower boundary of smouldering proposed in [6]. The interquartile ranges of the transient MCE for $MC > 50\%$ stayed outside of the smouldering boundary reported in [6]. For peat wetter than 160% MC, the MCE mean for not burning but drying peat which entails no decomposition reactions but mainly water evaporation, has a MCE value of 0.96, similar to that of flaming MCE marker (0.99) proposed in [10, 25].

Figure 14

Significant variations of the transient MCE were observed in smouldering experiments with peat $>25\%$ MC. This large variability was particularly intense during the ignition stage (see Fig. S6), which was also observed in a previous study [9]. In field studies, the judgement of a fire mode is primarily based on a MCE measured within a limited time period [6, 21], thus large uncertainty should be expected because a large-scale fire includes all the stages of Figure 14 at the same time but in different locations. While the experiments reported here observed one single smouldering front, field conditions include multiple smouldering fronts at different positions and at different times. This means that in the field, multiple drying, ignition, spreading and extinguishing stages are happening simultaneously over the large area where a peat fire is taking place. Shortly after the initiation of a peat fire, there is the expectation that the ignition stage reported in our experiment will dominate. Later on, the spreading

stage will dominate. But while one stage might dominate, the other stages will still be present albeit in different levels of importance.

4. Conclusion

Bench-scale experiments were carried out to investigate the mass loss, temperature profiles, real-time concentrations of 20 gas species, and size-fractionated particle mass from peat fires under different moisture conditions. For the first time, the combustion dynamics and transient emissions from flaming, smouldering and drying peat are investigated.

Moisture was found to affect both combustion dynamics and fire chemistry. Dry peat can sustain flaming combustion, and emit more fully oxidised gas species (for example, CO₂, NO₂ and SO₂) than smouldering peat. Flaming also generates soot particles less than 1 μm which are absent in smouldering. For smouldering, wet peat emits less CO₂, CH₄ and NH₃, but more CO, HCN and coarse particles (between 1 and 10 μm) than dry peat. When the peat becomes wet enough (moisture content larger than 160% for our samples), smouldering could not be sustained.

NH₃ emissions from smouldering peat were found to be 14-times larger than flaming peat, and 20 times larger than flaming fires of surface vegetation [9], making NH₃ the best candidate species for atmospheric detection of smouldering fires. This is also important for haze pollution because NH₃ favours the formation of particulate sulphate and nitrate which is one of the most important mechanisms forming haze [26, 27]. Our laboratory findings show that an increase of 160% moisture content can lead to an 84% decrease of the NH₃ EF. This shows that dry peatlands are hazardous in terms of fire spread and also emissions.

We examined the transient modified combustion efficiency (MCE) from all experiments and concluded that MCE is not an ideal fire regime indicator. MCE works for flaming, and smouldering dry peats with MC < 50%. However, MCE could not identify smouldering wet peat, especially for those with MC > 120%, and failed to differentiate flaming and drying peat. This work advances the scientific understanding of peat fires, and has the potential to accelerate mitigation strategies against this global-scale and unconventional source of pollutants.

Acknowledgements

The research has been funded by the European Research Council (ERC) Consolidator Grant HAZE (682587) and China Scholarship Council (CSC). The authors thank Muhammad Agung Santoso and Wuquan Cui from Imperial College London for valuable discussions and help in the lab.

References

- [1] M.R. Turetsky, B. Benscoter, S. Page, G. Rein, G.R. van der Werf, A. Watts, Global vulnerability of peatlands to fire and carbon loss, *Nat. Geosci.* 8 (2015) 11–14.
- [2] Y. Hu, N. Fernandez-Anez, T. E. Smith, G. Rein, Review of emissions from smouldering peat fires and their contribution to regional haze episodes, *Int. J. Wildland Fire*, 27 (2018) 293–312.
- [3] G. Rein, Smouldering Combustion (pp. 581-603), in: M.J. Hurley, D.T. Gottuk, J.R.H. Jr., K. Harada, E.D. Kuligowski, M. Puchovsky, J.L. Torero, J.M.W. Jr., C.J. Wieczorek (Eds.), *SFPE Handbook of Fire Protection Engineering*, Springer, 2016.
- [4] S.E. Page, F. Siegert, J.O. Rieley, H.-D. V. Boehm, A. Jaya, S. Limin, The amount of carbon released from peat and forest fires in Indonesia during 1997, *Nature* 420 (2002) 61–65.
- [5] G. Rein, N. Cleaver, C. Ashton, P. Pironi, J.L. Torero, The severity of smouldering peat fires and damage to the forest soil, *Catena* 74 (2008) 304–309.
- [6] C.E. Stockwell, T. Jayarathne, M.A. Cochrane, K.C. Ryan, E.I. Putra, B.H. Saharjo, A.D. Nurhayati, I. Albar, D.R. Blake, I.J. Simpson, E.A. Stone, Field measurements of trace gases and aerosols emitted by peat fires in central Kalimantan, Indonesia, during the 2015 El Niño, *Atmospheric Chem. Phys.* 16 (2016) 11711–11732.
- [7] G. Rein, S. Cohen, A. Simeoni, Carbon emissions from smouldering peat in shallow and strong fronts, *Proc. Combust. Inst.* 32 (2009) 2489–2496.
- [8] G. Rein, Smouldering fires and natural fuels, in: C. Belcher (Ed.), *Fire Phenomena and the Earth System*, Wiley and Sons, 2013.
- [9] Y. Hu, E. Christensen, F. Restuccia, G. Rein, Transient gas and particle emissions from smouldering combustion of peat, *Proc. Combust. Inst.* 37 (2018) 4035–4042.

- [10] S. Urbanski Wildland fire emissions, carbon, and climate: emission factors, *For. Ecol. Manage.* 317 (2014) 51–60.
- [11] U. Ballhorn, F. Siegert, M. Mason, S. Limin, Derivation of burn scar depths and estimation of carbon emissions with LIDAR in Indonesian peatlands, *Proc. Natl. Acad. Sci.* 106 (2009) 21213–21218.
- [12] X. Huang, G. Rein, H. Chen, Computational smouldering combustion: predicting the roles of moisture and inert contents in peat wildfires, *Proc. Combust. Inst.* 35 (2015) 2673–2681.
- [13] X. Huang, G. Rein, Downward spread of smouldering peat fire: the role of moisture, density and oxygen supply, *Int. J. Wildland Fire* 26 (2017) 907-918.
- [14] X. Huang, F. Restuccia, M. Gramola, G. Rein, Experimental study of the formation and collapse of an overhang in the lateral spread of smouldering peat fires, *Combust. Flame* 168 (2016) 393-402.
- [15] E. Christensen, Y. Hu, F. Restuccia, M. A. Santoso, X. Huang, G. Rein, Experimental Methods and Scales in Smouldering Wildfires, Chapter 19 in: ‘Fire effects on soils: State of the Art and Methods’, CSIRO, Australia, 2018. ISBN: 9781486308149.
- [16] N. Prat-Guitart, G. Rein, R. M. Hadden, C. M. Belcher, J. M. Yearsley, Propagation probability and spread rates of self-sustained smouldering fires under controlled moisture content and bulk density conditions, *Int. J. Wildland Fire* 25 (2016) 456- 465.
- [17] M.A. Santoso, X. Huang, N. Prat-Guitart, E. Christensen, Y. Hu, G. Rein, Smouldering Fires and Effects on the Soil: The State of the Art, Chapter 14 in: ‘Fire effects on soils: State of the Art and Methods’, Commonwealth Scientific and Industrial Research Organisation (CSIRO), Australia, 2018. ISBN: 9781486308149.
- [18] A. Usup, Y. Hashimoto, H. Takahashi, H. Hayasaka, Combustion and thermal characteristics of peat fire in tropical peatland in central Kalimantan, Indonesia, *Tropics* 14 (2004) 1–19.
- [19] C. Roulston, C. Paton-Walsh, T. E. L. Smith, É.-A. Guérette, S. Evers, C. M. Yule, G. Rein, G. R. Van der Werf, Fine particle emissions from tropical peat fires decrease rapidly with time since ignition, *J. Geophys. Res. Atmos.* 123 (2018) 5607–5617.
- [20] R. Hadden, Smouldering and self-sustaining reactions in solids: an experimental approach, PhD Thesis, The University of Edinburgh, Edinburgh, UK, 2011. <http://hdl.handle.net/1842/5587>.

- [21] T.E.L. Smith, S. Evers, C.M. Yule, J.Y. Gan, In situ tropical peatland fire emission factors and their variability, as determined by field measurements in Peninsula Malaysia. *Global Biogeochem Cycle*, 32 (2018) 18-31.
- [22] J. Yang, N. Liu, H. Chen, W. Gao, Smouldering and spontaneous transition to flaming over horizontal cellulosic insulation, *Proc. Combust. Inst.* 37 (2018) 4073-4081.
- [23] W.H. Frandsen, The influence of moisture and mineral soil on the combustion limits of smouldering forest duff, *Can. J. For. Res.* 17 (1987) 1540-1544.
- [24] K.M. Leung, R.P. Lindstedt, W.P. Jones, A simplified reaction mechanism for soot formation in non-premixed flames, *Combust. Flame* 87 (1991) 289-305.
- [25] S.K. Akagi, R.J. Yokelson, C. Wiedinmyer, M.J. Alvarado, J.S. Reid, T. Karl, J.D. Crouse, P.O. Wennberg, Emission factors for open and domestic biomass burning for use in atmospheric models, *Atmospheric Chem. Phys.* 11 (2011) 4039–4072.
- [26] J. Plautz, Piercing the haze, *Science*, 6407 (2018) 1060-1063.
- [27] X. Ye, Z. Ma, J. Zhang, H. Du, J. Chen, H. Chen, X. Yang, W. Gao, F. Geng, Important role of ammonia on haze formation in Shanghai, *Environ. Res. Lett.* 6 (2011) 024019.

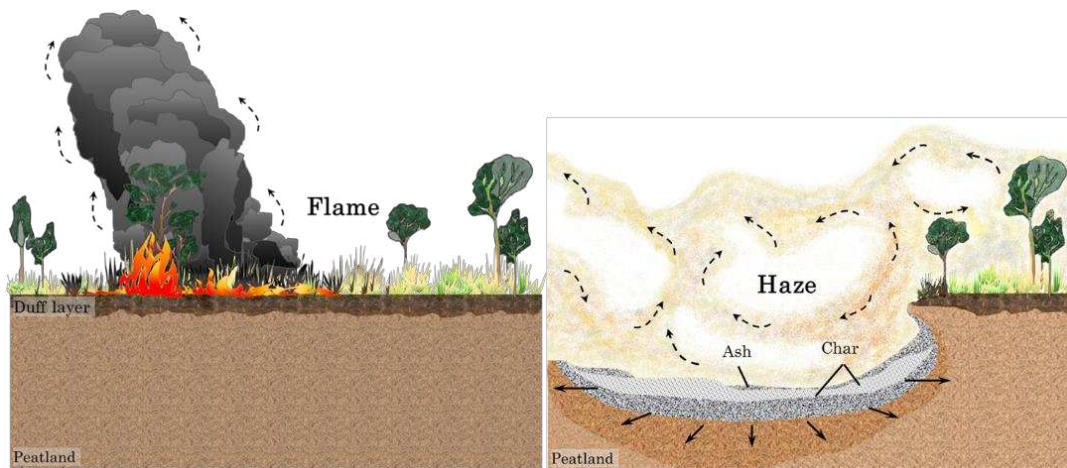


Figure 1 Schematics of a day-long peatland forest flaming fire (left), and the subsequent month-long smouldering peatland fire (right) [2].

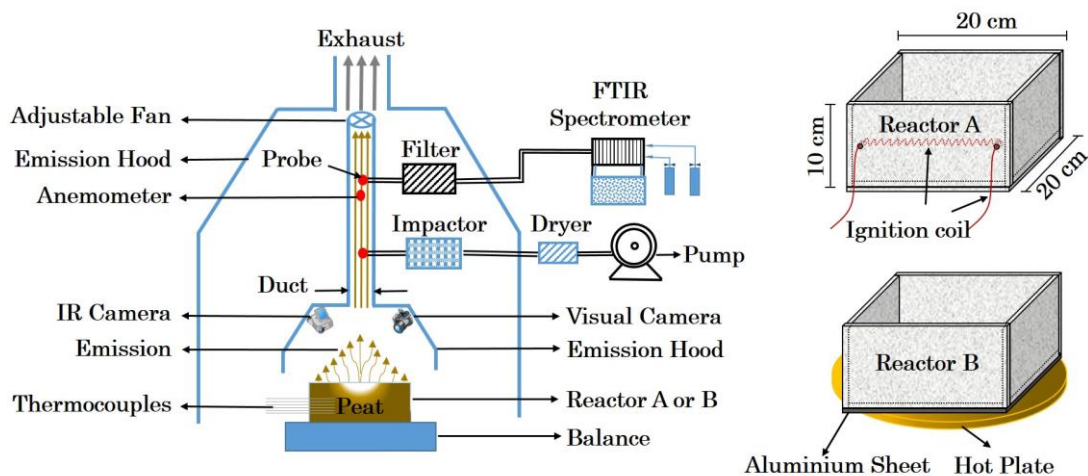


Figure 2 Schematic of the peat fire experiment set-up. Reactor A was used for all smouldering and flaming experiments; Reactor B was used for drying experiments.

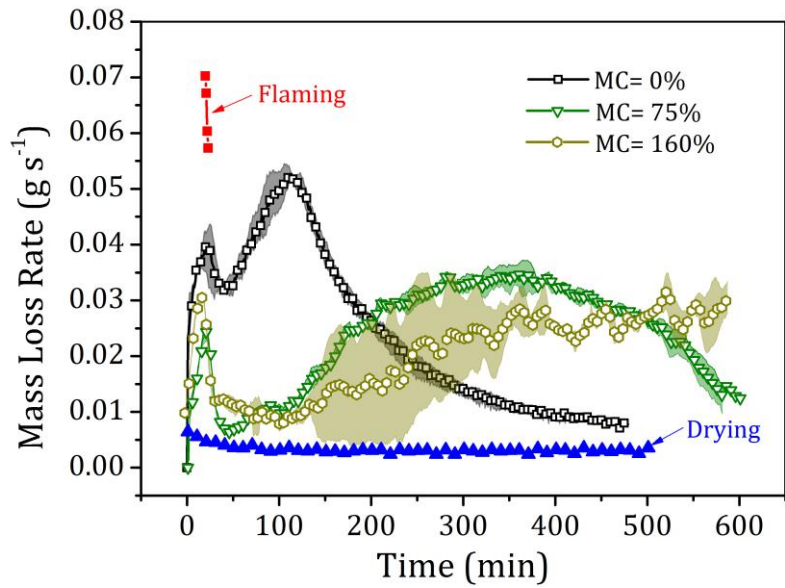


Figure 3 Evolution of mass loss rate measured during peat flaming, smouldering (at different MCs) and drying. Mass loss rate mean (line with symbol) and range (cloud) from the repeated experiments are shown.

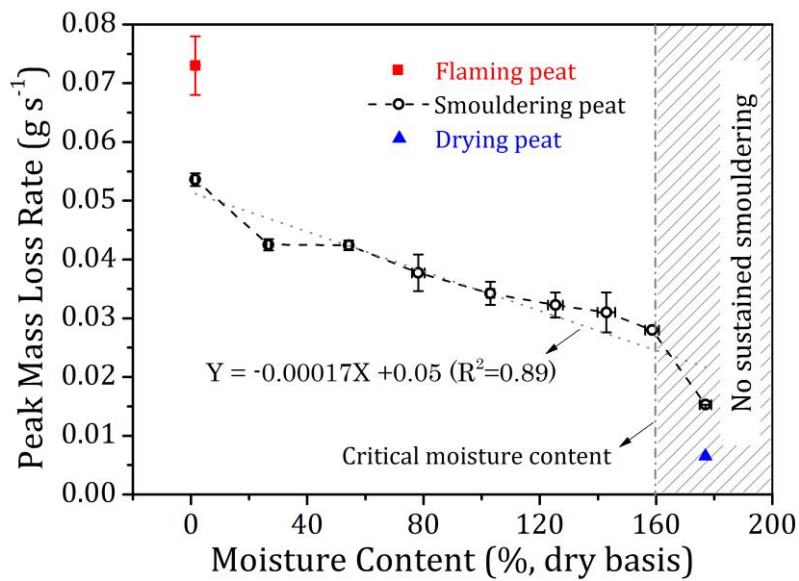


Figure 4 Peak mass loss rate for all peat fire experiments. 160% moisture content is the moisture content threshold for smouldering ignition. A linear regression was used to fit the mass loss rate data.

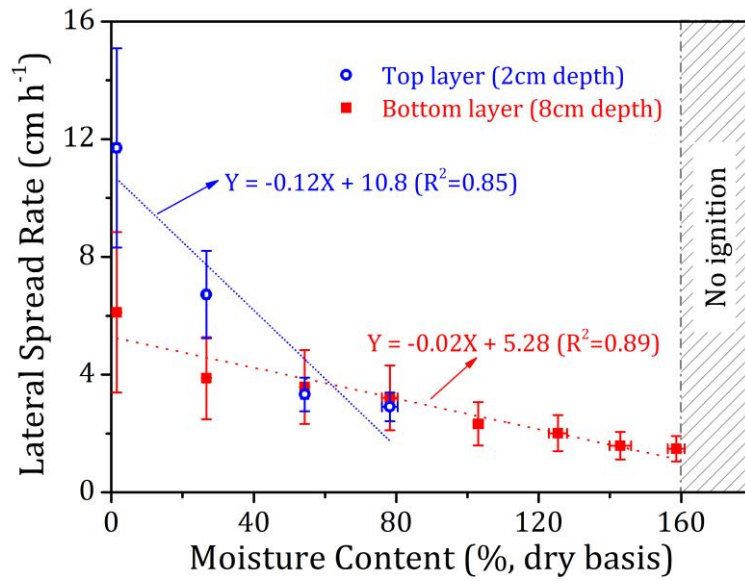


Figure 5 Spread rate of smouldering at different moisture contents as retrieved from the temperature profile.

It shows average spread rate at the top and bottom layers plus uncertainty. Linear regression fits the data.

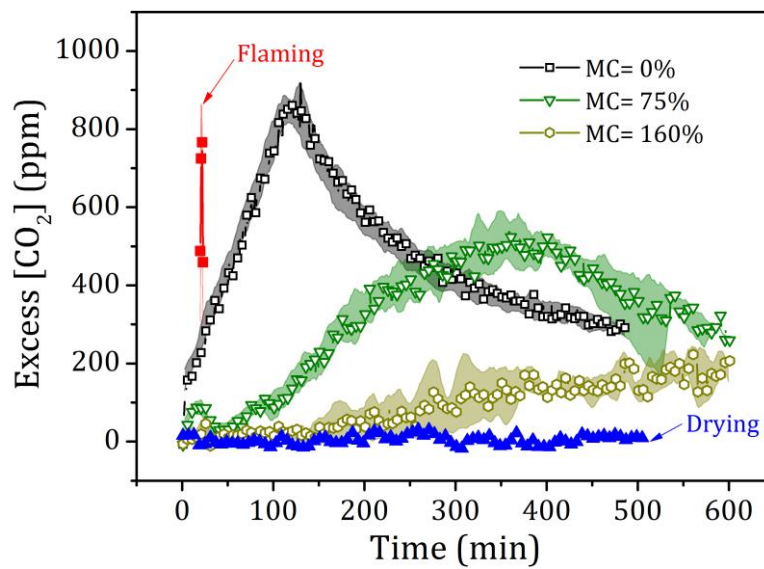


Figure 6 Evolution of CO₂ concentration during peat flaming, smouldering and drying stage. Mean value

(line with symbol) and the value range (cloud, smoothed) are shown.

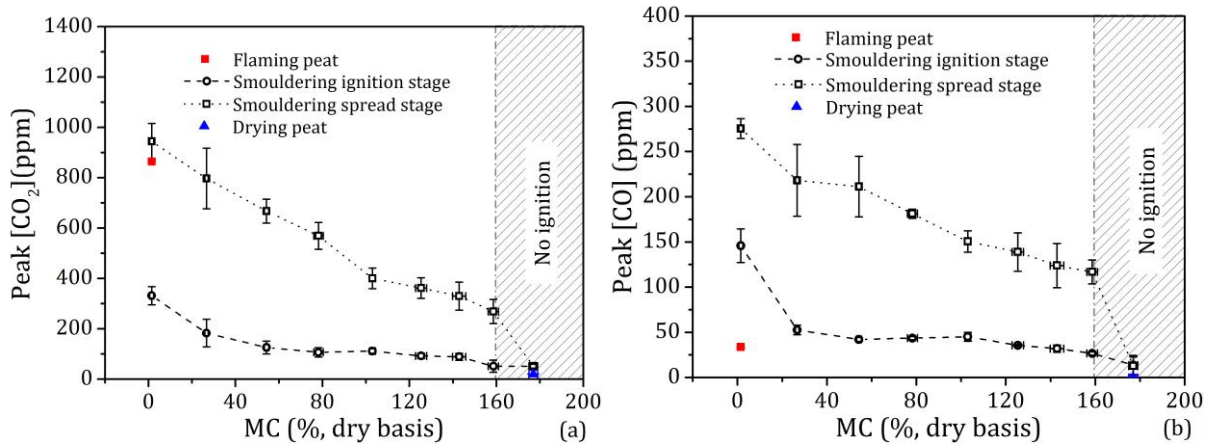


Figure 7 Peak values of CO_2 (a), and CO (b), from peat flaming, smouldering and drying experiments.

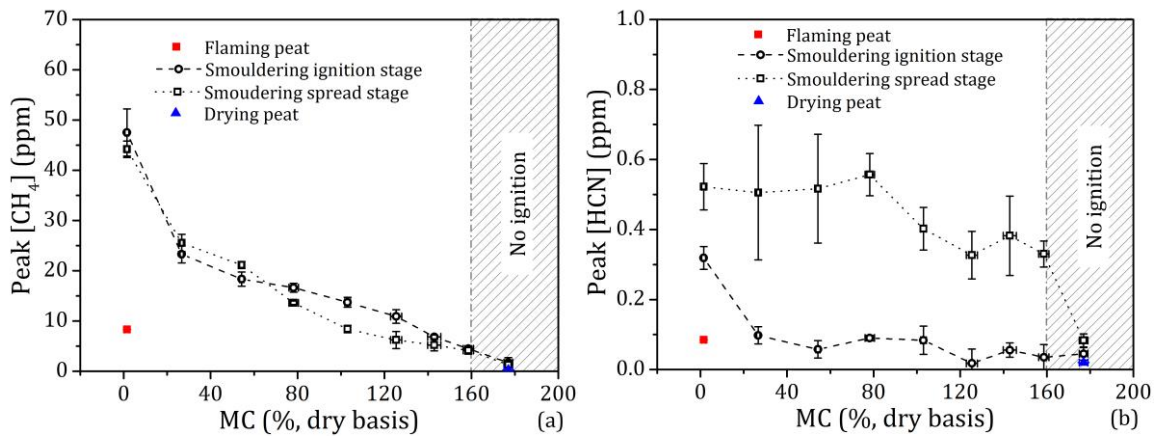


Figure 8 Peak values of CH_4 (a), and HCN (b), from peat flaming, smouldering and drying experiments.

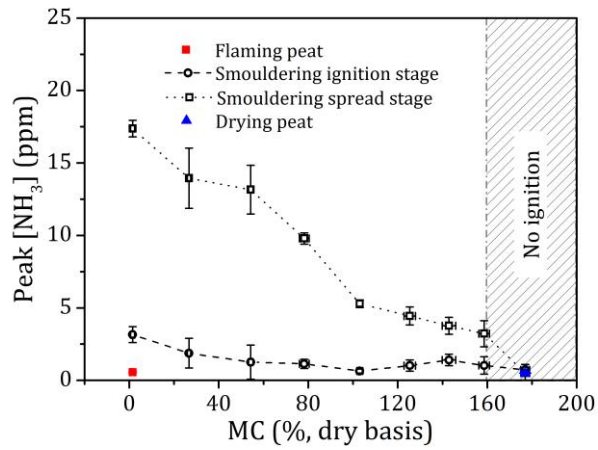


Figure 9 Peak values of $[NH_3]$ from peat flaming, smouldering and drying experiments.

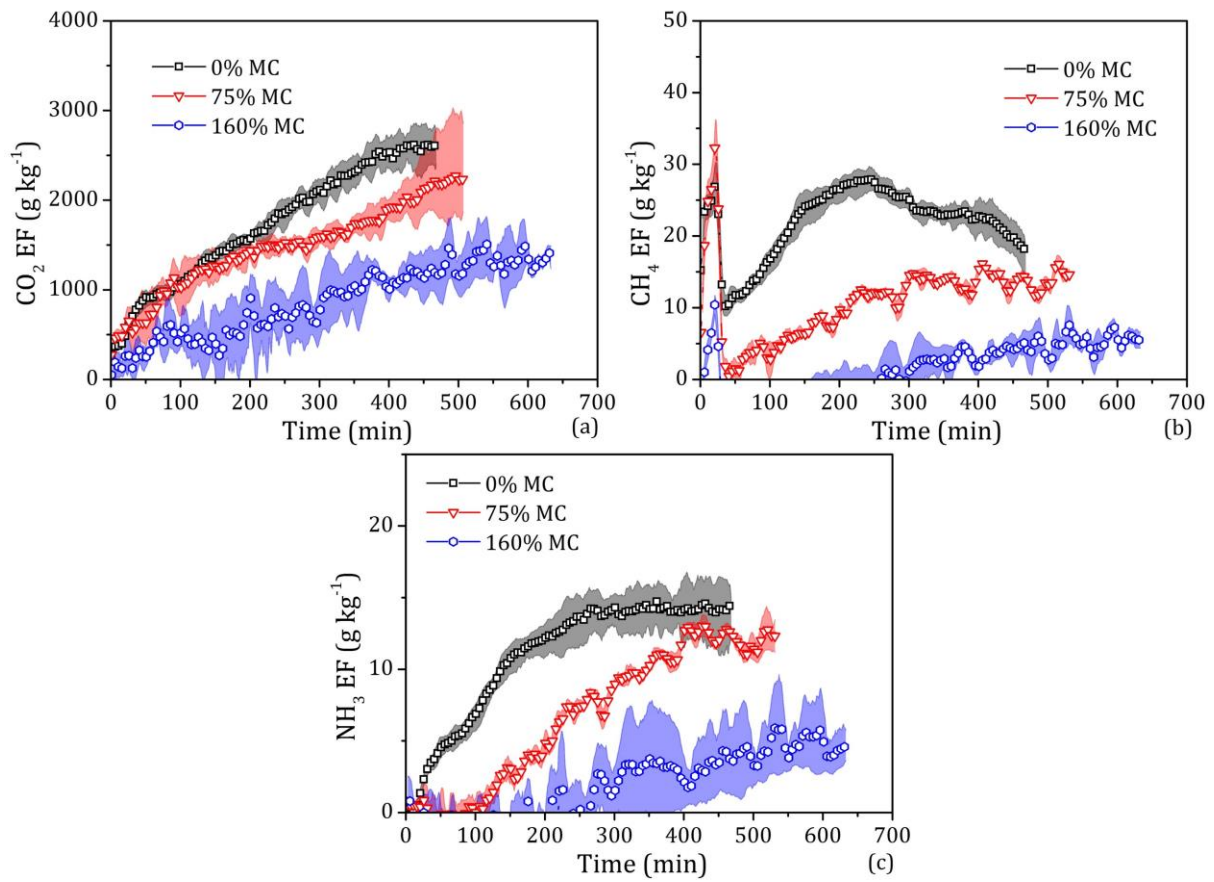


Figure 10 Transient CO_2 (a), CH_4 (b), and NH_3 (c) emission factor from smouldering peat fires with 0%, 75% and 160% targeted moisture contents. Emission factor mean (line with symbol) and range (cloud) from the repeated experiments are shown.

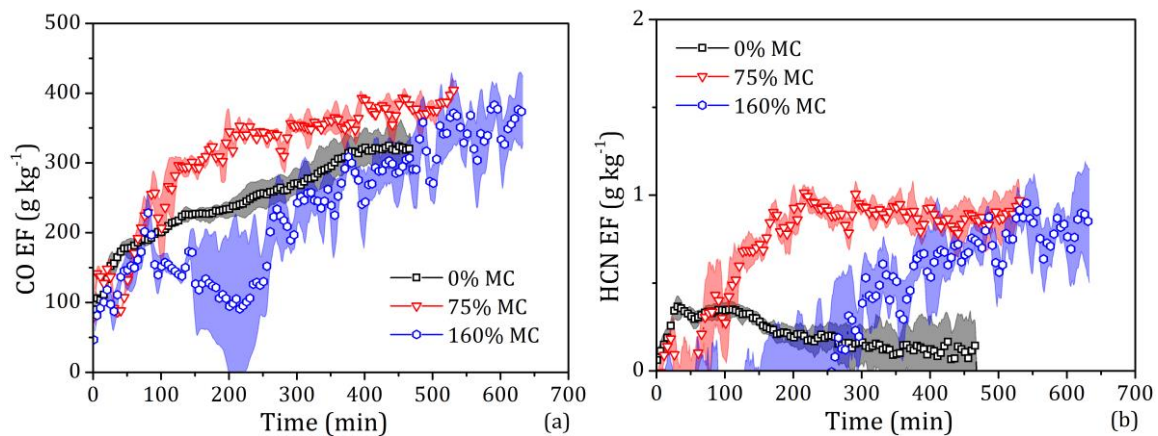


Figure 11 Transient CO (a), and HCN (b) emission factor from smouldering peat fires with 0%, 75% and 160% targeted moisture contents. Emission factor mean (line with symbol) and range (cloud) from the repeated experiments are shown.

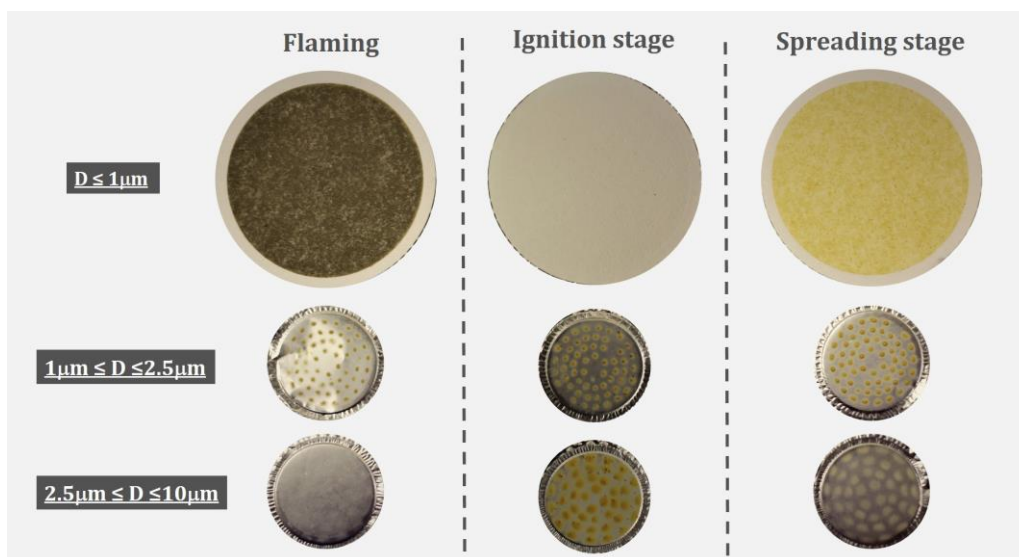


Figure 12 Filters and the collected size-fractionated particles from the particulate matter impactor. Particles emitted from the flaming, smouldering ignition and spreading of dry peat are shown.

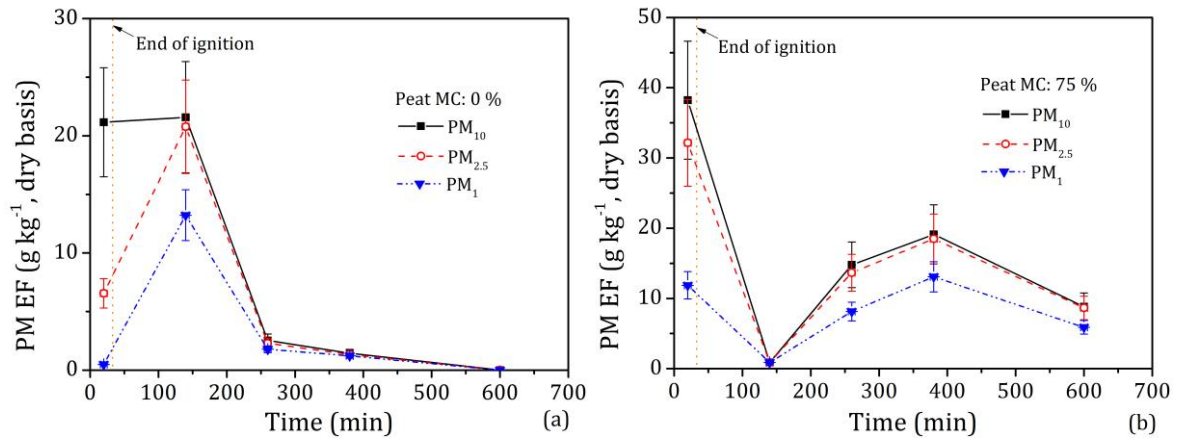


Figure 13 Transient EF of PM₁₀, PM_{2.5} and PM₁ from smouldering during ignition and spread stages with MC of 0% (a) and 75% (b). Error bars were determined from uncertainty propagation detailed in [8].

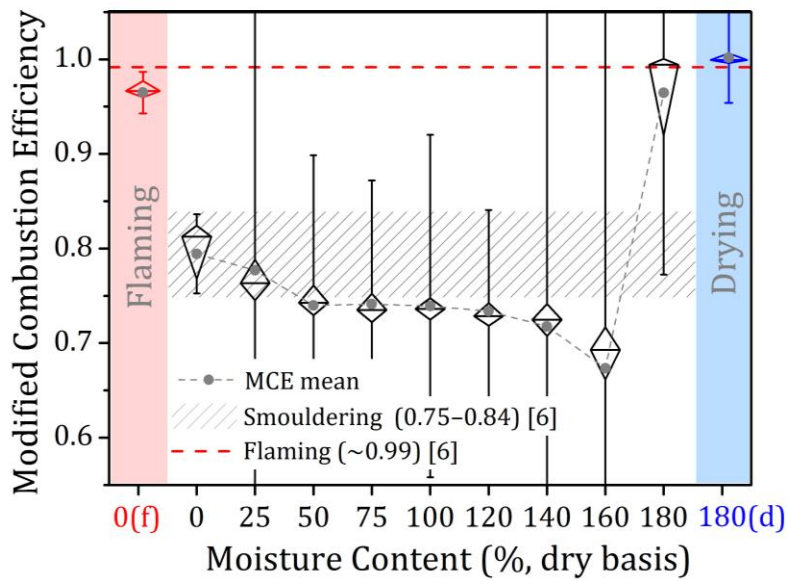


Figure 14 Boxplot of MCE from all peat fire experiments. Each data point is transient MCE through lower quartile (25th percentile), the median (50th percentile) and upper quartile (75th percentile). “0(f)” on the x-axis refers to flaming peat, “180(d)” refers to drying peat. The error bars show one standard deviation above and below the mean.